RSC Advances

RSC Publishing

PAPER

View Article Online
View Journal | View Issue

Cite this: *RSC Adv.*, 2013, **3**, 26290

Cysteamine hydrochloride protected carbon dots as a vehicle for the efficient release of the anti-schizophrenic drug haloperidol†

Sunil Pandey,‡* Ashmi Mewada,‡ Mukeshchand Thakur,‡ Arun Tank and Madhuri Sharon*

Received 30th April 2013
Accepted 8th October 2013

DOI: 10.1039/c3ra42139b

www.rsc.org/advances

The use of phenylalanine derived non-toxic carbon dots (C-dots) as a vehicle for the delivery of widely used anti-psychotic drug haloperidol (HaLO) is described in the present research work. The C-dots were found to have remarkable optical properties and to exhibit bright green fluorescence under UV light ($\lambda_{ex} = 365$ nm). The UV-Vis spectrum of the C-dots exhibits peaks at 232 and 276 nm confirming their synthesis in solution. The size of the C-dots was found to be in the range of 5–10 nm, as confirmed by Field Emission Scanning Electron Microscopy (FE-SEM). Cysteamine hydrochloride (CysHCl) was used as a non-toxic linker to functionalize the purified C-dots before grafting HaLO on the surface to facilitate the controlled release under physiological conditions. A constant release of HaLO was achieved for more than 40 h, which followed the Hixson–Crowell model under standardized conditions. The C-dot–CysHCl–HaLO conjugate was found to have a much higher compatibility with MDCK cells at pH 7.2 in comparison to bare HaLO.

Introduction

Controlled drug release of potential therapeutic agents is one of the major milestones to be conquered by designing smart vehicles equipped with drugs and navigational molecules for targeted delivery. Metal nanoparticles, owing to their tunable size and optical properties, have been the favourite ingredient for delivering a plethora of therapeutic agents to different targets including solid tumors.[1,2] These nanoparticles can circumvent the most common problems in chemotherapy, such as the inferior dispersion of the drugs in body fluids, killing non-specific cells due to lack of targeting, development of drug resistance due to repeated administration of drugs in high concentrations, and poor retention and permeation of the drugs inside the cells or tumors.[3]

In the past few years, major emphasis has been given to the delivery of anti-psychotic drugs such as haloperidol, due to the potential toxicity and side effects associated with such therapeutic agents.[4] Depot formulations of drugs for the treatment of psychosis such as schizophrenia have several important features over conventional oral drug delivery formulations (tablets, capsules, aerosols) such as:

(1) High absorption of drugs by the concerned tissues or other targets.

(2) Lower extra pyramidal side effects due to the reduction in the administration of drugs.

(3) Less frequent intake of drugs up to once a week or two, unlike with capsules and tablets which require to be taken 3–4 times a day.

Over the years after their fabulous discovery in 2004,[5] C-dots have gained interest because of their high biocompatibility,[6] unique optical properties,[7] high solubility in water-based formulations and easy surface functionalization protocols which can also be used as linkers for the attachment of therapeutic agents. The properties of the C-dots can be exploited to replace metal containing semiconductor quantum dots such as CdTe, CdS, and CdSe which involve extremely inimical precursors[8,9] as well as high temperatures for their synthesis.[5,9] The typical photoluminescence (PL) properties of C-dots in the near-infrared region (NIR) can also be used as a combinatorial technique for the photo-thermal therapy of solid tumors.[10,11] Moreover, their fluorescence and high quantum yield can also be used for biological imaging.[12,13] There are a variety of protocols for the facile production of C-dots.[14–18] There are very few reports on the nanoparticle-mediated drug delivery of haloperidol,[19,20] a widely used drug for the treatment of schizophrenia. To the best of our knowledge, there are no reports on the delivery of haloperidol using C-dots as drug delivery vehicles.

In the present work, phenylalanine was used as a precursor to fabricate highly fluorescent C-dots that were then grafted with HaLO for controlled drug release. Cysteamine

N.S.N. Research Center for Nanotechnology and Bionanotechnology, Ambernath, MS, India. E-mail: gurus.spandey@gmail.com; sharonmadhuri@gmail.com; Tel: +91 9004024937

† Electronic supplementary information (ESI) available. See DOI: 10.1039/c3ra42139b

‡ Authors have equal contribution in this work.

hydrochloride was used to functionalize the as-prepared C-dots for the formation of stable bonds to facilitate the controlled release. After the surface functionalization with cysteamine hydrochloride, HaLO was grafted on the surface of the functionalized C-dots and its release kinetics was studied using statistical models under physiological conditions as well as the impact of the C-dot–CysHCl–HaLO conjugate on endothelial cells.

Experimental

Materials and methods

All the chemicals used in the experiments were of analytical grade and used as received. Prior to use, the glassware was washed with diluted chromic acid followed by nanopure water. All the reagents were prepared using nanopure water.

Synthesis and purification of C-dots

2 g of phenylalanine (Sigma-Aldrich, USA) was subjected to microwave-assisted pyrolysis for 30 s. To this pyrolysed material, 3 ml of absolute ethanol and 1 M NaOH mixture (1 : 1 ratio) were added and further subjected to microwave heating for 30 s. The resulting solution was cooled and its fluorescence under UV light (365 nm) was observed after addition of 1 ml of 1 M NaOH.

In order to get pure C-dots, the obtained solution was transferred to a pre-activated dialysis bag (MW cutoff 12–14 kD, pore size of 2.4 nm) and dialysed against nanopure water for 24 h under stirring conditions. The sample was analyzed spectrophotometrically.

Functionalization of C-dots with cysteamine hydrochloride (CysHCl)

An aqueous stock solution (3000 ppm) of CysHCl (Sigma-Aldrich, USA) was prepared by dissolving 30 mg of CysHCl in 10 ml of nanopure water. 83 μl of the CysHCl solution was added to 2 ml of purified C-dots and the total volume was made 5 ml with nanopure water maintaining the concentration at 50 ppm.

Attachment of haloperidol to the C-dot–Cys complex

A stock solution of haloperidol (Sigma-Aldrich, USA) was prepared by dissolving 1 mg of drug in 1 ml of nanopure water. For the synthesis of the above complex, 50 μl of the prepared drug stock solution was added to 5 ml of the C-dot–CysHCl conjugate to maintain the concentration of the added drug at 10 μg ml^{-1}. This solution was subjected to mild stirring at 28 ± 2 °C for 2 h.

Drug loading efficiency

5 ml of the C-dot–CysHCl–HaLO conjugate was dialyzed against nanopure water for 4 h and the concentration of unbound HaLO was calculated using UV-Vis spectroscopy at a wavelength of 245 nm. The Drug Loading Efficiency (DLE) was calculated using the following equation:

$$\mathrm{DLE}\,(\%) = \frac{\text{theoretical amount of drug loaded} - \text{free drug}}{\text{theoretical amount of drug loaded}} \times 100 \quad (1)$$

Cytotoxicity

The cytotoxicity of the C-dots and the C-dot–drug complex was studied on MDCK cells using the MTT assay which is based on the mitochondrial enzyme mediated conversion of pale yellow MTT to violet colored crystals of formazan. Cells were seeded (5×10^5 ml^{-1}) in 96-well plates and incubated at 37 °C and 5% CO_2 for 24 h. After satisfactory growth, the medium was replaced with test solutions of C-dots, the C-dot–CysHCl–HaLO complex and free haloperidol, and incubated further for 48 h. Later, these solutions were replaced with a solution of MTT (200 μg ml^{-1}). Cells were incubated for 2.5 h at 28 ± 2 °C to initiate the formation of formazan. After completion of the reaction, the medium was replaced with 200 μl of DMSO (Sigma, USA). This complex was agitated moderately to dissolve the formazan crystals. Finally, the dissolved formazan in DMSO was transferred to fresh 96-well plates and read on a microplate reader (Thermo, USA) at 570 nm.

Drug release and kinetics of haloperidol

In order to elucidate the drug release profile of HaLO under physiological conditions (pH 7.2 at 37 °C) in phosphate buffered saline (PBS), 3 ml of C-dot–CysHCl–HaLO conjugate was sealed in a dialysis bag (MW cutoff 12–14 kD, pore size 2.4 nm) and kept in a 100 ml of the PBS solution heated at 37 °C under mild intermittent stirring. 3 ml samples were collected at 30 min intervals for 4 h and then at 24 h intervals for 3 days. The removed sample was replaced by PBS every time. The concentration of the released drug was calculated using a standard calibration curve at a wavelength of 245 nm.

To analyze the drug release profiles, suitable statistical models were used as in our previous work.[1,2]

Characterization

The spectral properties of the C-dots were studied by UV-Vis spectroscopy (Lambda-25, Perkin-Elmer, USA) and fluorescence spectroscopy (Perkin-Elmer, USA) using a standard quartz cuvette having a path length of 1 cm. 250 nm was selected as the excitation wavelength. Morphological details of the C-dots were obtained using Field Emission Scanning Electron Microscopy (FE-SEM) (Zeiss Microimaging GmbH, Germany) and High Resolution Transmission Electron Microscopy (HRTEM) (Zeiss Microimaging GmbH, Germany). The purified C-dots were loaded on a silicon substrate and on a coated copper grid for the FE-SEM and TEM analysis, respectively. Energy Dispersive Analysis of X-ray (EDAX) was performed to find out the elemental composition of the sample using FE-SEM (Carl Zeiss Microimaging, GmbH, Germany) equipped with an Oxford EDAX analyzer, UK. The crystallinity of the C-dots was studied using X-ray diffraction (XRD) (Phillips, The Nederland). For the analysis, the samples were coated on a glass coverslip and dried under ambient conditions. Raman spectra were recorded using

a Jobin-Yvon Labram spectrometer. Fourier transformed infrared (FTIR) spectroscopy (Brucker) studies were performed within the spectral window of 500 to 4000 cm^{-1}. For the thermogravimetric analysis (TGA), 20 mg of the sample was placed in a TGA cell (Perkin-Elmer, Diamond, USA) and heated to 900 °C at a heating rate of 20 °C min^{-1} in an atmosphere of N_2 gas.

Results and discussion

After microwave assisted heating of the alkaline solution of phenylalanine; there were three important observations which confirmed the formation of C-dots:

(1) A change in colour from colourless to dark brown due to the carbonization of the phenylalanine.

(2) A sharp peak and a shoulder at 232 and 276 nm, respectively (Fig. 1a), in the UV-vis spectra.

(3) Bright green fluorescence under UV-light (365 nm) (inset of Fig. 1a).

All the above properties are due to the specific surface functionalization and energy traps present in the C-dots. The dual peak in the UV range is a signature marker of C-dots.[13,21] The sharp peak at 232 nm is originated due to the $\pi \rightarrow \pi^*$ transition of the electrons of C=C present in the C-dots, and the other feeble peak at 276 nm is due to the $n \rightarrow \pi^*$ transition of electrons associated with carbonyl groups.[22] The absence of background absorbance in the visible region indicates the absence of other carbonaceous materials which usually absorb at higher wavelengths.[23] Another signature marker is the peak at 468 nm in the PL spectra (λ_{ex} = 250 nm), arising from the unique functionalization and surface properties of the C-dots[21] (Fig. 1b).

For the efficient use of C-dots as drug delivery vehicles, the surface of the C-dots was modified with CysHCl, an ideal linker for the attachment of anti-cancer drugs.[2] After the surface modification with CysHCl, the peaks exhibited by pure C-dots (232 and 276 nm) shifted to 224 and 277 nm, followed by a decrease in the intensity of the peaks (Fig. 1a). These alterations in the spectra may arise due to the formation of weak interactions between CysHCl and the oxygenated moieties associated with the C-dots, which are considered to be crucial in the origin of their optical properties.[21] Further, after the attachment of HaLO to the surface of the C-dots, the peaks became feebler due to masking of the functional groups. Compared to the peaks observed for the C-dot–CysHCl conjugate, there is a slight blue shift of 1 nm (from 224 to 223 nm) and a few small peaks at 273, 330 and 375 nm are due to HaLO and the C-dot–CysHCl–HaLO conjugate. Photoluminescence (PL) (Fig. 1b) is another celebrated attribute of C-dots and it is sensitive to surface modifications.[14] The origin of PL is believed to be associated with surface functionalization and energy traps.[24] However, the exact mechanism of PL is still unknown. All the samples were excited at 250 nm after a few initial trials. Pure C-dots exhibit a peak at 468 nm with intense green color under UV light (inset Fig. 1a). After attachment of CysHCl and HaLO, the peaks shifted to 472 and 463 nm, respectively, along with a substantial decrease in the intensity of the peaks as shown in Fig. 1b. PL of the C-dots became blue under UV light (365 nm) after the surface modification with CysHCl and again turned green when HaLO was added.

The FE-SEM image (Fig. 2a) shows the presence of roughly spherical C-dots of size 5–10 nm. A HRTEM image showing a spherical C-dot of 5 nm is displayed in the inset of Fig. 2a with a typical lattice constant of 0.3 nm, as previously reported.[25] Fig. 2b displays the EDAX spectrum of the C-dots which shows the presence of carbon along some impurities. The X-Ray Diffraction (XRD) pattern (Fig. 2c) displays a characteristic peak at $2\theta = 25.67°$ and a weak peak at $2\theta = 42.17°$, which are

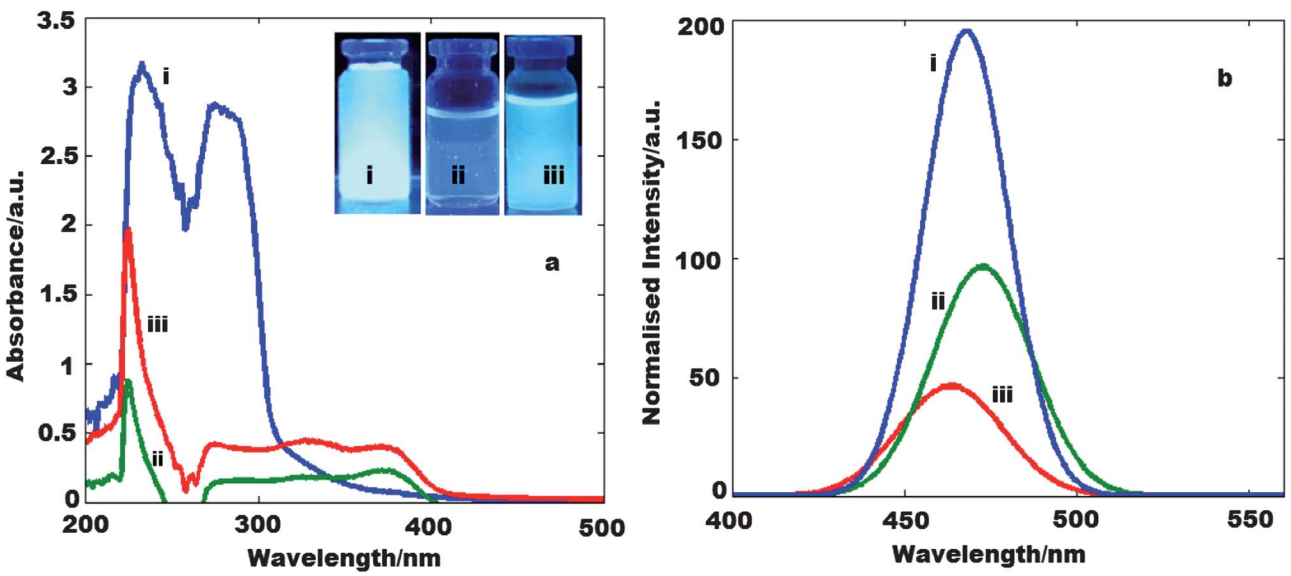

Fig. 1 (a) UV-vis spectra of C-dots, the C-dot–CysHCl complex and C-dot–CysHCl–HaLO labeled as i, ii and iii, respectively; the inset shows the fluorescence of the samples under UV light; and (b) photoluminescence spectra of the same samples.

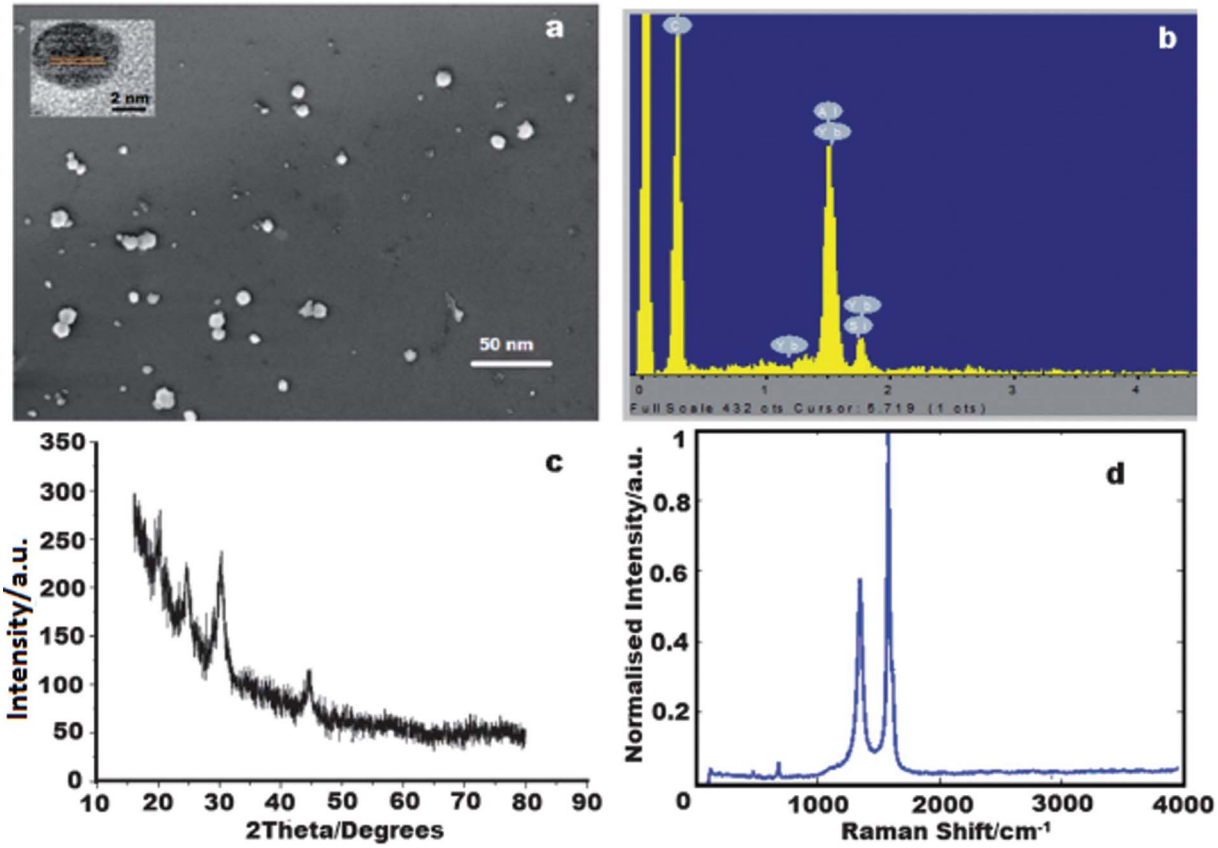

Fig. 2 (a) FE-SEM image of C-dots displaying a size range between 5 and 10 nm; the inset shows a HRTEM image of a single C-dot exhibiting the typical lattice constant of C-dots (0.3 nm); (b) EDAX spectrum of C-dots; (c) XRD pattern of C-dots; and (d) Raman spectrum displaying the signature peaks for C-dots.

assigned to the (002) and (101) diffraction patterns of graphitic carbon. The peak at 25.67° is due to an interlayer spacing of ~3.77 Å, higher than that between the (002) planes in bulk graphite *i.e.* 3.44 Å.[26]

The Raman spectra of the phenylalanine derived C-dots is shown in Fig. 2d. The G-band at 1582 cm^{-1} and the D-band at 1356 cm^{-1} indicate the presence of amorphous carbon nanomaterials in the form of C-dots.[27]

Attachment studies were performed using Fourier transform infrared (FTIR) spectroscopy. The FTIR spectrum of bare C-dots (Fig. 3a) show bands at 582 cm^{-1} and 989 cm^{-1} for the alkene C–H bending vibrations, whereas the multiple broad bands from 1000–1250 cm^{-1} correspond to the C–O and C–O–C stretch vibrations on the surface of the passivated C-dots. The IR band at 1410 cm^{-1} is attributed to a few other exposed functional groups such as alkane C–H, CH_2 and CH_3 bends, and alkene C=C stretch. The band at 2897 cm^{-1} corresponds to the amine N–H bend. The strong band at 3350 cm^{-1} indicates the presence of the O–H stretch due to the NaOH mediated hydroxyl functionalization and due to the suspension of C-dots in an aqueous solution. The FTIR spectrum of bare CysHCl is given in the ESI, Fig. S1†. Upon attachment of CysHCl to the C-dots, the FTIR spectrum reveals a band at 605 cm^{-1}, which is a shifted C-dot band indicating some modifications on the alkene C–H bend.

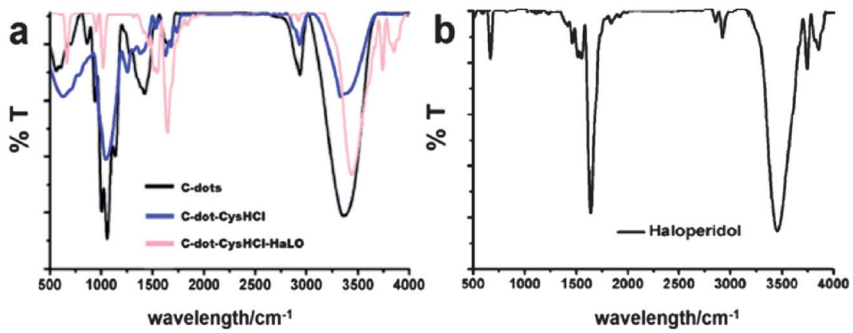

Fig. 3 FTIR spectra of (a) C-dots, C-dot–Cys HCl, and C-dot–Cys HCl–HaLO conjugate showing possible interactions and (b) bare haloperidol in aqueous solution.

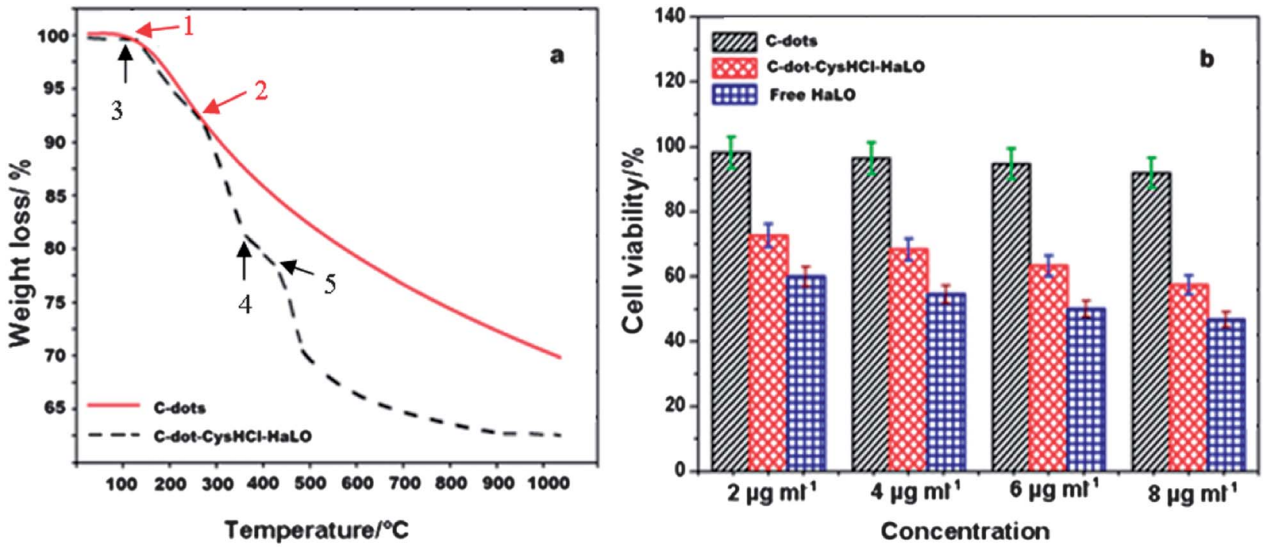

Fig. 4 (a) TGA of C-dots synthesized using phenylalanine and the C-dot–CysHCl–HaLO conjugate; (b) cytotoxicity of C-dots, the C-dot–CysHCl–HaLO conjugate and free HaLO on MDCK cells.

Table 1 Inimical effects of the conjugate and pure C-dots on MDCK cells[a]

	Viability (%)		
Concentration (μg ml^{-1})	C-dots	C-dot–CysHCl–HaLO conjugate	Free HaLO
2	98.2 ± 4.1	72.54 ± 2.9	60 ± 3.3
4	96.5 ± 4.1	68.31 ± 2.1	54.6 ± 3.3
6	94.8 ± 3.2	63.24 ± 1.9	50.1 ± 3.2
8	92 ± 2.1	57.45 ± 1.9	46.8 ± 3.3

[a] Values expressed as mean ± standard deviation.

The strong band at 1044 cm^{-1} for the C–N stretch indicates the formation of a covalent bond between the C-dot passivated surface and the amino group of CysHCl since there is a significant shift in the 939 cm^{-1} band of CysHCl. Further, the strong band at 2920 cm^{-1} suggests a thiol (–SH) interaction between the CysHCl and the amine N–H since there is significant shift in the amine stretch of the C-dots. The strong band at 3350 cm^{-1} is due to the O–H stretch from the aqueous suspension. The FTIR spectrum of the bare haloperidol molecule (Fig. 3b) shows a band at 673 cm^{-1} for the alkane CH_2 and C–H bends. The bands at 1543–1620 cm^{-1} refer to the C–H plane and the amino N–H bend. The band at 2901 cm^{-1} indicated =CH stretches whereas those at 3446–3853 cm^{-1} show aqueous O–H stretches. The FTIR spectrum of the final complex (Fig. 3a), C-dot–CysHCl–HaLO, shows the presence of a strong new band at 1639 cm^{-1} which indicates the formation of a covalent imine bond (–C=N–) stretch. It is worth noticing that there is shift in the 1044 cm^{-1} band of the C-dot–CysHCl complex which may be also taking part in the bond formation.

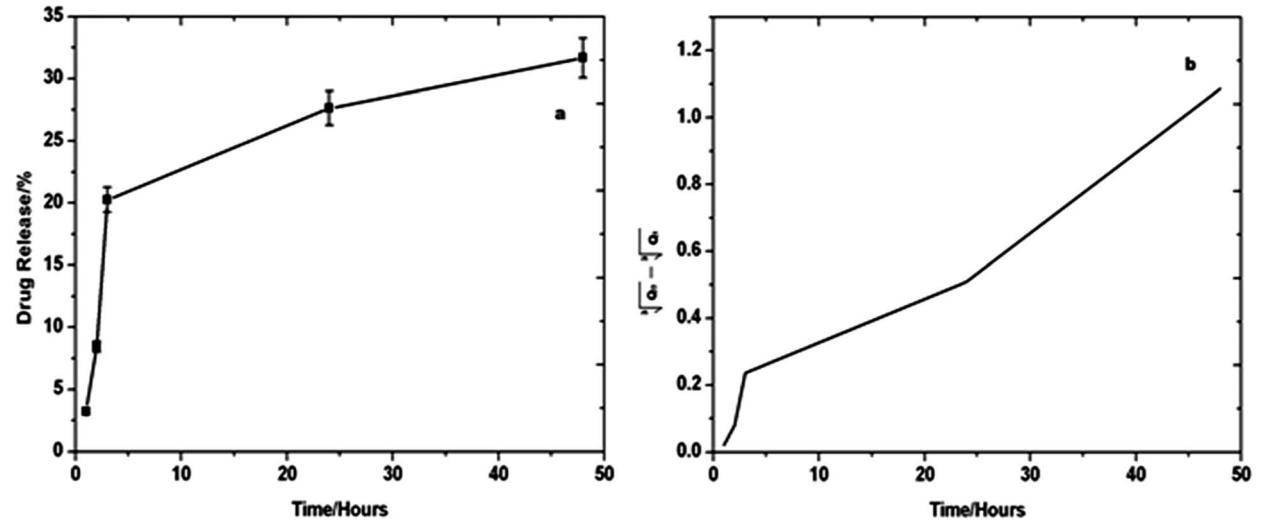

Fig. 5 (a) Percentage release of HaLO with respect to time; (b) drug release profile of HaLO using the Hixson–Crowell model under physiological conditions.

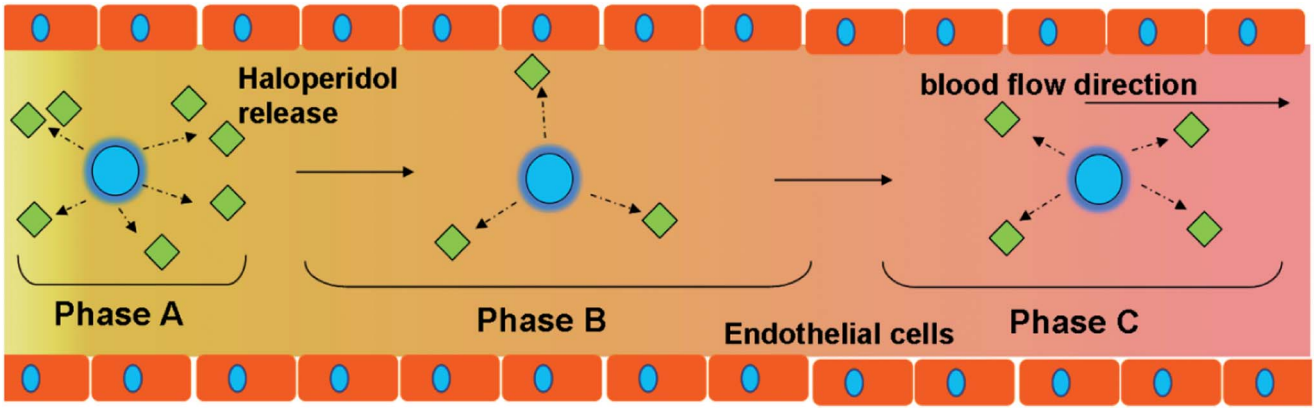

Fig. 6 Schematic depicting the different phases of the release profile of haloperidol from the C-dot–CysHCl–HaLO complex: Phase A, Phase B and Phase C as a function of time.

This is further supported by the decrease in the intensity of the peak at 2933 cm^{-1} due to the involvement of the N–H stretch in the imine bond formation. Since the final conjugate was suspended in water, the multiple peaks around 3441–3858 cm^{-1} are attributed to the O–H stretch. The other bands at 660 cm^{-1} depict the alkane CH_2 and C–H bends whereas those between 1012 and 1520 cm^{-1} correspond to the C–O and C=C stretches.

To further understand the attachment, thermogravimetric analysis (TGA) was performed on bare C-dots and the C-dot–CysHCl–HaLO conjugate, Fig. 4a. In pure C-dots, there are two important steps of weight loss at 120 °C (7%, marked 1) and 300 °C (13%, marked 2) which may be due to the loss of water molecules associated with the surface of the C-dots and a gradual loss of oxygen bearing moieties including CH, respectively. The C-dot–CysHCl–HaLO conjugate, on the other hand, exhibits multiple weight losses. The initial loss is assigned to water molecules as explained above. Further depletion in the weight at 120 °C (7%, marked 3), 380 °C (19%, marked 4) and 495 °C (28%, marked 5) are due to the multiple binding between the drug and CH and other functional groups. A loss of weight was completed at 1000 °C, which indicates high thermal stability as well as stable interactions within the conjugate.

C-dots have become a favourite ingredient in biological applications due to their exceptional biocompatibility.[13,28] In our case, the impact of C-dots and the C-dot–CysHCl–HaLO conjugate on MDCK cells was found to be negligible. At the measured concentrations (2–8 μg ml^{-1}), the percentage cell survival was found to be ~90% (Fig. 4b). The slight decrease in the survival of the cells after the interaction with pure C-dots may be due to the alkalinity of the C-dots as well as the presence of traces of metal ions. There are many reports on the evaluation of the toxicity of C-dots protected with a plethora of surface functionalizing agents.[29,30] When we compared our results to previous findings, C-dots were found to be exceptionally biocompatible with normal cells. This proves the efficacy of CysHCl as an ideal linker for drug delivery.

Bare HaLO in similar concentrations was found to be considerable toxic as shown in Table 1. The IC50 of HaLO was calculated to be 6 μg ml^{-1} whereas the maximum effect (57.45%) of the C-dot–CysHCl–HaLO conjugate was found to be 8 μg ml^{-1}. The C-dot–CysHCl–HaLO conjugate displays a considerable lower toxicity, as evident from Fig. 4b. A possible explanation for the reduction in the inimical effects is explained as follows:

(i) The conjugation of HaLO with the biocompatible C-dots.

(ii) Controlled release of drug under physiological conditions due to the porous nature of the C-dots, as well as the impact of CysHCl as the linker.

(iii) C-dots can get selective access to cells due to their large interactions with biological membranes,[30] avoiding unwanted internalization.

The drug loading efficiency was calculated to be 75.24%. Fig. 5a shows the drug release profile as a function of time under physiological conditions (pH 7.2, 37 °C). Previous studies on the release of encapsulated HaLO in PLGA nanoparticles[19,20] reported diffusion as the mode of drug release. In order to comprehend the deeper intricacies of the drug release, we have divided the release process in three phases (Fig. 6):

(i) A rapid release phase was observed in the initial 4–5 h during which HaLO diffuses due to a concentration gradient (ΔG is negative).

(ii) Initiation of sustained release (6–24 h), during which the drug is released at a lower rate under physiological conditions.

(iii) Sustained release was achieved within 24–40 h. This phase is usually slow and over a long period of time. After this phase is over, almost all the drug is released at a slow rate and the nanoparticles are ready to be metabolized.

This ideal release pattern was also observed by several other researchers[19] using polymeric nanoparticles, and hence, the efficacy of tiny C-dots as a drug delivery vehicle is justified. For validation of the actual drug release pattern or kinetics, we used different statistical models to assess the type of release profile under the present conditions. Among the four most widely used models (Zero Order, First Order, Higuchi and Hixson–Crowell), we found that the HaLO release follows the Hixson–Crowell model (Fig. 5b) based on the highest correlation value (R_2) obtained. The Hixson–Crowell model is dominant in types of drugs where the particle size varies in terms of diameter and surface area.[31] The Hixson–Crowell model is mostly followed by powders (granular haloperidol in our case).

Drugs that follow this model present prolonged effects like HaLO.

Conclusion

C-dots, due to their excellent optical properties including surface passivation, can act as nano-carriers for the delivery of the most widely used anti-psychotic drug, haloperidol. We found the C-dots to have a high drug loading capacity, possibly due to their porous nature and surface orchestration during alkali assisted microwave heating. As confirmed by optical spectroscopy, FTIR and TGA, there are multiple interactions between the conjugates ensuring their stability. Finally, the conjugate was found to have an ideal drug release profile in PBS (pH 7.2) at 37 °C and to follow the Hixson–Crowell model. Recently, carbon-dots have been used as drug delivery vehicles in cancer therapeutics,[32–34] and the present report provides an insight into the delivery of therapeutics such as anti-psychotic drugs. This might also pave the way into the theranostic-based application of carbon-dots.

Acknowledgements

Authors are indebted to the authorities of N.S.N. Research Center for funding the projects. We are also thankful to TIFR, Mumbai and IIT Bombay, SAIF department-Mumbai for carrying out the FTIR and FE-SEM characterization. We thank the concerned reviewers for their valuable comments and suggestions.

Notes and references

1 S. Pandey, G. Oza, A. Mewada, R. Shah, M. Thakur and M. Sharon, *J. Mater. Chem. B*, 2013, **1**, 1361.
2 S. Pandey, R. Shah, A. Mewada, M. Thakur, G. Oza and M. Sharon, *J. Mater. Sci.: Mater. Med.*, 2013, **24**, 1671.
3 R. K. Jain and A. Stylianopoulos, *Nat. Rev. Clin. Oncol.*, 2010, **7**, 653.
4 D. Dubois, *Curr. Opin. Pediatr.*, 2005, **17**, 227.
5 X. Xu, R. Ray, Y. Gu, H. J. Ploehn, L. Gearheart, K. Raker and W. Scrivens, *J. Am. Chem. Soc.*, 2004, **126**, 12736.
6 S. N. Baker and G. A. Baker, *Angew. Chem., Int. Ed.*, 2010, **49**, 6726.
7 J. H. Shen, Y. H. Zhu, X. L. Yang and C. Z. Li, *Chem. Commun.*, 2012, **48**, 3686.
8 S. C. Ray, A. Saha, N. R. Jana and R. Sarkar, *J. Phys. Chem. C*, 2009, **113**, 18546.
9 A. B. Bourlinos, A. Stassinopoulos, D. Anglos, R. Zboril, M. Karakassides and E. P. Giannelis, *Small*, 2008, **4**, 455.
10 S. F. Lim, R. Riehn, W. S. Ryu, N. Khanarian, C. K. Tung, D. Tank and R. H. Austin, *Nano Lett.*, 2006, **6**, 169.
11 L. Tang, R. Ji, X. Cao, J. Lin, H. Jiang, X. Li, K. S. Teng, C. M. Luk, S. Zeng, J. Hao and S. P. Lau, *ACS Nano*, 2012, **6**, 5102.
12 J. C. G. Esteves da Silva and H. M. R. Goncalves, *TrAC, Trends Anal. Chem.*, 2011, **30**, 1327.
13 A. Mewada, S. Pandey, S. Shinde, N. Mishra, G. Oza, M. Thakur, M. Sharon and M. Sharon, *Mater. Sci. Eng., C*, 2013, **33**, 2914.
14 S. Pandey, A. Mewada, G. Oza, M. Thakur, N. Mishra, M. Sharon and M. Sharon, *Nanosci. Nanotechnol. Lett.*, 2013, **5**, 775.
15 L. Cao, X. Wang, M. J. Meziani, F. Lu, H. Wang, P. G. Luo, Y. Lin, B. A. Harruff, L. M. Veca, D. Murray, S. Y. Xie and Y. P. Sun, *J. Am. Chem. Soc.*, 2007, **129**, 11318.
16 A. R. Selvi, D. Jagadeesan, B. S. Suma, G. Nagashankar, M. Arif, K. Balasubramanyam, M. Eswaramoorthy and T. K. Kundu, *Nano Lett.*, 2008, **8**, 3182.
17 Q. L. Zhao, Z. L. Zhang, B. H. Huang, J. Peng, M. Zhang and D. W. Pang, *Chem. Commun.*, 2008, 5116.
18 H. Liu, T. Ye and C. Mao, *Angew. Chem., Int. Ed.*, 2007, **46**, 6473.
19 A. Budhian, K. Winey and S. Siegel, *J. Microencapsulation*, 2005, **22**, 773.
20 Y. H. Cheng, L. Illium and S. S. Davis, *J. Controlled Release*, 1998, **55**, 203.
21 L. Haitao, K. Zhenhui, L. Yang and L. Shuit-Tong, *J. Mater. Chem.*, 2012, **22**, 24175.
22 Z. Luo, Y. Lu, L. A. Somers and A. T. Charlie Johnson, *J. Am. Chem. Soc.*, 2009, **131**, 898.
23 Y. Dong, J. Shao, C. Chen, H. Li, R. Wang, Y. Chi, X. Lin and G. Chen, *Carbon*, 2012, **50**, 4738.
24 Z. H. Kang, Y. Liu and S. T. Lee, *Nanoscale*, 2011, **3**, 777.
25 Y. Li, Y. Hu, Y. Zhao, G. Shi, L. Deng, Y. Hou and L. Qu, *Adv. Mater.*, 2011, **23**, 776.
26 B. Y. Pan, J. C. Zhang, W. Q. Shen, Z. W. Zhang, Y. G. Fang and M. H. Wu, *New J. Chem.*, 2010, **34**, 591.
27 M. S. Dresselhaus, A. Jorio, M. Hofmann, G. Dresselhaus and R. Saito, *Nano Lett.*, 2010, **10**, 751.
28 N. Puvvada, B. N. P. Kuma, S. Konar, H. Kalita, M. Mandal and A. Pathak, *Sci. Technol. Adv. Mater.*, 2012, **13**, 045008.
29 S. T. Yang, X. Wang, H. Wang, F. Lu, P. G. Luo, L. Cao, M. Meziani, J. H. Liu, Y. Liu, M. chen, Y. Huang and Y. P. Sun, *J. Phys. Chem. C*, 2009, **113**, 18110.
30 Y. Wang, P. Anilkumar, L. Cao, J. H. Liu, P. G. Luo, K. N. Tackett 2nd, S. Sahu, P. Wang, X. Wang and Y. P. Sun, *Exp. Biol. Med.*, 2011, **236**, 1231.
31 A. W. Hixson and J. H. Crowell, *Ind. Eng. Chem.*, 1931, **23**, 923.
32 L. Zhou, Z. Li, Z. Liu, J. Ren and X. Qu, *Langmuir*, 2013, **29**, 6396.
33 S. Pandey, M. Thakur, A. Mewada, D. Anjarlekar, N. Mishra and M. Sharon, *J. Mater. Chem. B*, 2013, **1**, 4972.
34 Q. Wang, X. Huang, Y. Long, X. Wang, H. Zhang, R. Zhu, L. Liang, P. Teng and H. Zheng, *Carbon*, 2013, **59**, 192.

